

Surface Roughness Effect on the Fatigue Lifetime of SLM Stainless Steel (316L) Parts.

Khalid Mustafa Alrbaey¹, Nori Abosag²

1- Higher Institute of Science and Technology- Surman.

2- Higher Institute of Engineering Technology- Gharyan.

المخلص :

كل المواد الهندسية تتمتع بخواص ميكانيكية خاصة بها مثل المتانة، الاجهاد، الانفعال، الصلابة و غيرها. هذا ومن الملاحظ إن هذه الخواص تتأثر مباشرة بجودة الاسطح وخشونتها وخصوصا في حالة الاحمال المتكررة مثل اختبار الكلال. ونظراً للتقدم العلمي في مجال الصناعة الحديثة أصبحت تقنيات التصنيع بالليزر تلعب دوراً مهماً في تصنيع القطع المعقدة، والتي لاتزال تعاني من بعض العيوب مثل خشونة الاسطح للمنتج والذي يتراوح من 10 الى 30 ميكرون . في هذا البحث تم إنتاج العينات المصنوعة من مادة الستانلسستيل (316 L) وتجهيزها على آلة الليزر (SLM 125). حيث تم تقييم الأداء الميكانيكي للعينات تحت اختبار الكلال بعدما تعرضت العينات الى مرحلتين من مراحل تحسين خشونة السطح وهما على الترتيب (إعادة معالجة السطح بالليزر والتلميع بواسطة التحليل الكهربائي). تم اختبار العينات باستخدام آلة اختبار الكلال (HSM 20) ومقارنة النتائج علي منحنى (S-N). حيث أظهرت النتائج تحسناً في الأداء الميكانيكي للعينات ليصل إلى حوالي 50% مع تحسن في خشونة السطح للعينات.

Abstract:

In the realm of scientific materials, all kinds of metals have natural properties such as mechanical strength, strain, and hardness etc. However, the surface roughness of a material can have effects on product quality and mechanical performance, such as fatigue, creep and corrosion resistance. Additive manufacturing technologies such SLM has offered a new design possibility in terms of industrial application, but the product still suffer from poor surface roughness which ranges from 10-

30microns. Therefore, good control of the SLM process and post-process is necessary to decrease the range of surface roughness. Moreover, knowledge about dynamic mechanical behavior is still lacking due to process parameter changes.

The main aim of this study is to assess the performance(fatigue lifetime) of SLM stainless steel (316L) parts subjected to two different stages of surface finish method, namely laser re-melting and electro-polishing. The samples under various surface toughness and after applying the above stages of surface finish were tested by using a fatigue tester (HSM 20).Also the S-N curve of the samples was plotted and the results reveal about 50% of total improvement in fatigue lifetime.

1- Introduction:

Failure of a material occurs when a large amount of stress is concentrated at a fixed point, although the maximum stress applied at that point may be below the yield stress. This phenomenon is known as fatigue. In such case, the tensile stresses at a microscopic point are applied leading to encourage cracks to initiate starting from the edge and continue increasing. Once the stresses have been initiated, this helps to develop the crack until the reduction of section and has lost its potential to carry the applied load. It is worth mentioning that all materials suffer fatigue but that this varies. Endurance limit stress is known as fatigue limit. For instance, mild steel stress levels are set at a level below which the fatigue fracture will not occur. The steel sample has a fatigue limit of 414 M pa, whereas non-ferrous materials, such as aluminium alloys are unlikely to suffer from such a phenomenon, but there is still no specific limit ascertained [1][2]. Figures 1 & 2 below present this information.

The actual stress range for materials like mild steel can be maintained below the endurance limit. Moreover, the design for specific number of stress variations can be developed if a certain portion of materials can be replaced at the stage of stress variation

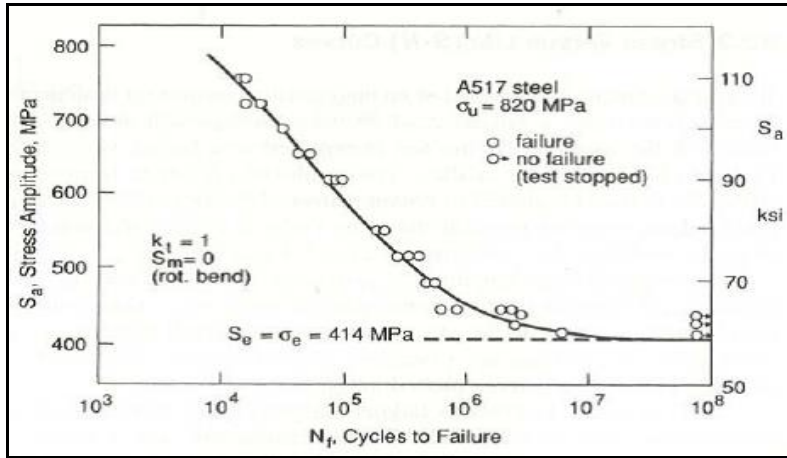


Figure 1: Stress-life time curve for ferrous material[3]

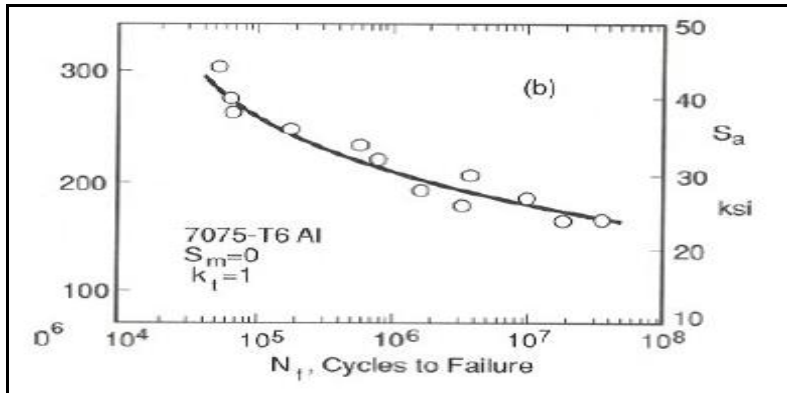


Figure 2: Stress lifetime curve for nonferrous material

The use of this method may be of benefit in aircraft construction as aluminum is commonly used in this construction. Results from the fatigue tests are important and are used by engineers to design parts to attain fatigue strength. Such results may, however, not be applicable, when designing for an infinite lifetime[4].

1.2- Fatigue Crack Growth (FCG):

The data gained from the Fatigue crack growth graph is important to explain the main force behind its behaviour. This data is commonly represented on a log plot of crack growth rate (da/dN) versus ΔK (stress intensity factor ($\Delta K=K_{max}-K_{min}$)) as shown in (figure 3).

The development of the analytical models is based on three different regions of the FCG curve, which denote the empirical data. The 'near threshold' region with a very slow crack growth is the region (I). In this region, the growth of a crack will not occur fast because the amount of driven force is below the threshold value. Although this region is highly influenced by the applied load it is also highly sensitive to the parts features and test environment such as material microstructure, grain size and operating temperature. Whereas region (II) is an intermediate zone presented as a line relation on the crack growth curve. Region (III) is where the higher growth rate will occur leading to unbalanced final fracture. This occurs when the remaining cross-section of the tested material will not be able to carry the applied load although the maximum stress (K_{max}) equals the fracture toughness of the material (K_c). [5]

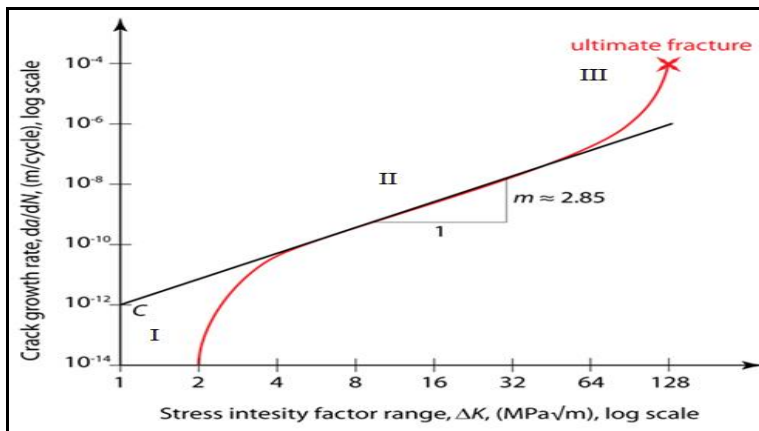


Figure 3: Typical Fatigue Crack Growth Curve Showing Three Regions.

All regions of the typical range of FCG data have been represented through various relationships, which have been developed over the years. To represent the linear region of the curve, the Paris Equation is the simplest relationship that was developed in 1963:

$$\frac{da}{dN} = C (\Delta K)^n$$

The applications used today are still applying this original model represented above, where the crack length is given by 'a', the empirical parameters are denoted by 'C' which is calculated from a curve fitting to test data, while 'n' stays in the range 3 to 5 for metals. The mean stress effects, threshold behaviour (region I), the instability asymptote (region III) and fatigue closure effects were studied based on this original model to develop more advanced versions of the Paris equation.[6][7]

For instance, For man and Walkers modified this relationship by introducing a factor dependent on (1-R). Where $R = \sigma_{min}/\sigma_{max}$ or K_{min}/K_{max} , in the denominator to introduce flexibility for mean stress as linear model using the load ratio(R).

$$\frac{da}{dN} = C \left[\frac{\Delta K}{(1-R)^{1-m}} \right]^n$$

The empirical factors such as 'C', 'n' and 'm' are determined from the curve of FCG test data which was achieved at the various load ratios[8].

1.3- Surface Roughness Effect on Fatigue Life time :

Surface roughness parameters are describing all surface texture of parts in terms of various parameters. But the most commonly used parameter is the arithmetic average roughness (Ra), which is referred to the centre line average. Whereas (Rt) is the distance between the highest peak and the lowest valley in the same track [9].

Generally, fatigue behaviour has been proven to vary under different surface finishes for traditional material, but the knowledge for additive manufacturing is not fully studied because the process is changeable. For instance, surface carburization and scale defects are usually found on local forging metal which leads to decreased fatigue lifetime, specifically in high cycle fatigue region(HCF). However,the surface roughness of low cycle fatigue regions has less effect. On the other hand, the effect of the as-forged surface finish will be reduced through surface cleaning treatments such as, sand blasting. These techniques will remove scale defects with some of decarburized layers in order to improve the surface properties. In some cases, compressive residual stresses can be maintained at the top of surface, which it could be recommended especially for fatigue application.

The literature related to the effects of machined surface topography and integrity of fatigue lifetime was reviewed by Novovic et al. ,who found that the most commonly applied parameter was R_a ,to describe the fatigue behaviour of material,but specimens with the same R_a value showed fatigue results with a typical 20% scatter. Thus , R_t could be preferred in comparison to R_a , when determining the fatigue performance, as they successfully represented worst surface defects and allowed the initial crack growth[10].

In addition, a comparative study has been done by Spierings et al. ,to compare the behavior of conventional material and SLM (Selective Laser Melting) fabricated material under dynamic fatigue test. The results revealed that the fatigue lifetime for SLM SS316L samples is about 25%, less than that of the conventional materials at lower stress, even under differing surface conditions for the two tests. Also the endurance limit for SLM samples was demonstrated as 20% lower than conventional materials at lower stress. At higher stress(higher amplitudes) the materials showed a similar lifetime[11].

2- Description of the apparatus :

The induction squirrel cage motor was used to drive the fatigue tester HSM20 with a specific speed of 3000rpm. This is

shown in the Figure 4. A 220V single phase power supply was provided. A counter mechanism is fitted at one side of the motor, which has the ability to record 7 figure members. A fixture is connected at its end to the shaft. A spherical ball bearing is positioned in the loading device with a micro switch. When the fracture occurs, the motor is automatically switched off by the micro switch. The process was carried out with the help of a fatigue tester, which is designed to be positioned on the bench. A standard specimen is provided for the apparatus. These specimens come with standard dimensions of (1x 10 x 100) mm as demonstrated below.

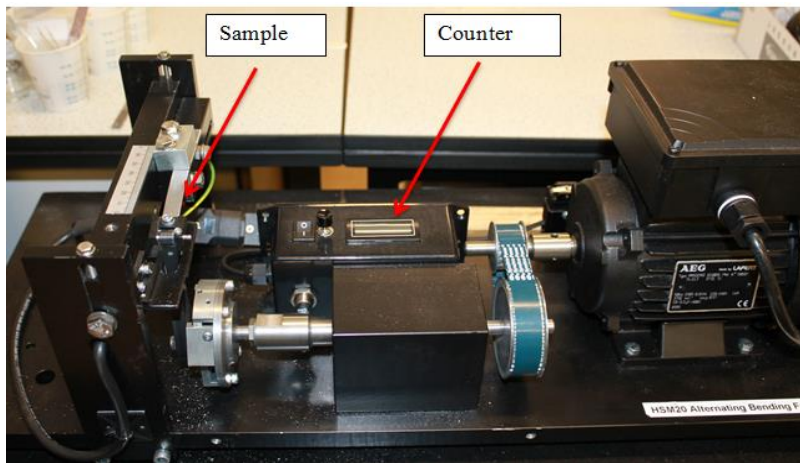


Figure 4: Fatigue tester HSM20.

3- Experimental Procedure:

SLM 125 was used to generate specimens in vertical orientation, through specific steps, start by CAD model (Solid Works) and turned to require end geometry with a specific dimension (100 x 10 x 1) mm. Thus, the manufacture parts have been completed.

The CAD model and the final manufacture parts (Figure 5 & 6) are showed as the following:

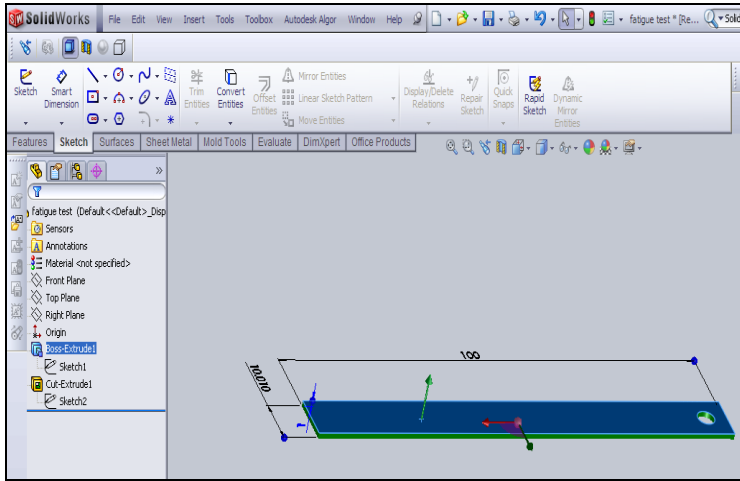


Figure 5: Shows CAD model part.

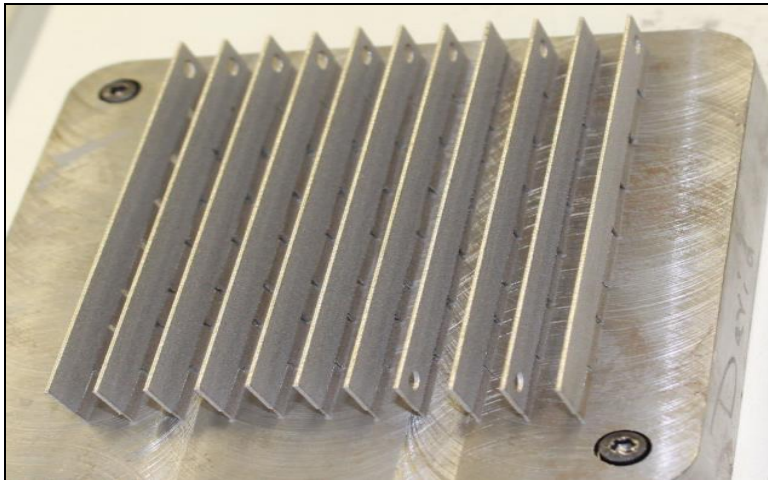





Figure 6: Shows the fatigue samples fabricated by SLM(125).

Twenty seven samples were manufactured and divided into three groups. Also surface roughness was measured for all three sets of SLM samples, as fabricated, Re-melted samples and Electro-polished samples, in order to detect the manner in which the fatigue lifetime is affected by the surface roughness.

The table below demonstrated details of the fabricated samples through different stages of surface improvement.

Table 1: Shows specimens' profile(1x 10 x100) with the most important parameters for surface finish improvement.

	Part	Process parameters &Comments
As fabricated		<ul style="list-style-type: none"> • Laser power 200 watt • Scan speed 480mm/s • Layer thickens 50 μm • Exposure time 100 μs • Average roughness (Ra) 9.15 $\mu\text{m} \pm 10\%$
Re -melted		<ul style="list-style-type: none"> • Grid scanning method • Laser power 180 watt • Scan speed 400 mm/min • Beam spot size 1mm • Hatch spacing 0.4mm • Focal distance 128 mm • Average roughness(Ra) 1.4 $\mu\text{m} \pm 20\%$
Polished		<ul style="list-style-type: none"> • Potential cell 4 volts • Ethylene 200 (ChCl:EG) as solution • Experimental time 45 min • Temperature 40 C° • Average roughness(Ra) 0.35 $\mu\text{m} \pm 15\%$

The experimental was carried out through three stages as :

- 1- Generate fatigue test on SLM samples(as fabricated material).
- 2- Generate fatigue test after Re-melted (as first stage to improve surface roughness).
- 3- Generate fatigue test after re-melted and polished (as final finishing stage).

The effects of the comparable rough surface quality on the specimen's lifetime were studied through this experiment. Cyclic cantilever bending was imposed on the samples at 1400 rpm, 20Hz when loading.

In order to clarify this process in a simple way, the processes of cyclic cantilever bending conditions were functional on the Y-axis to apply reversing stresses on each sample. Thus, the recorded results were taken for the total number of cycles to failure of each applied amplitude stress. Not all samples showed fatigue failure, especially those exposed to less than 500 M Pa of amplitude stress. Therefore, the test is usually terminated after about 2×10^5 cycles.

Then S-N relationship is ascertained for various specific loading amplitudes and created for the materials tested under varying stress amplitude. The stress amplitude is denoted by 'S', while the number of cycles are denoted by 'N'.

As the fatigue performance is severely affected by the amplitude of cyclic loading, the minimum peak stress divided by the maximum peak stress is the R ratio value, which is used to express the amplitude, as shown in the following figure.

- Stress ratio $R = \sigma_{min} / \sigma_{max}$.

It is most common to test at R ratio of -1 and kept constant.

- Stress range $\Delta\sigma = \sigma_{max} - \sigma_{min}$.

- The mean stress
$$\sigma_m = \frac{\sigma_{max} + \sigma_{min}}{2}$$

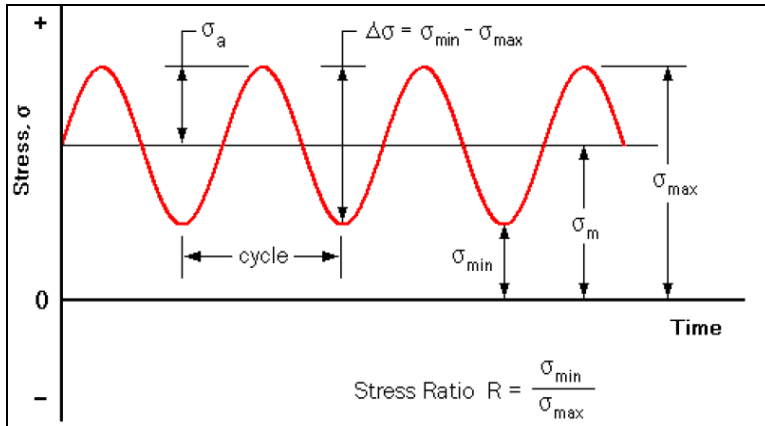


Figure 7 : Schematic of cyclic loading.

The schematic of the fatigues test configuration is presented in the Figure 8 below.

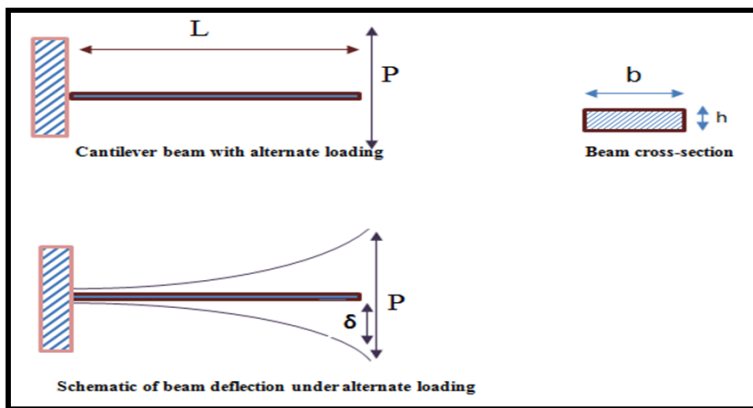


Figure 8: Schematic of the fatigue test configurations.

The following table presents the fixed conditions of tested samples;

Table 2: Specification of tested samples :

Specifications	Samples
The length of beam (L) = mm	40 mm
The width of Cross-section (b) = mm	10.1 mm
The height of cross section (h) = mm	1.02 mm
The second moment of area $I = \frac{b h^3}{12} =$	0.9197mm ⁴

The beams cantilever analysis is dependent on the followed equations;

$$\text{A) Beam deflection } \delta = \frac{P L^3}{3EI} \quad (mm)$$

Where δ is cantilever beam deflection, and E is Young's modulus (200) MPa and P is the load performed to generate specific deflection.

B) The maximum bending moment occurs at the fixed end is

$$M_{\max} = PL \quad (Nm)$$

C) The maximum bending stress at the fixed end [12]

$$\sigma_{\max} = \frac{M_{\max} Y_{\max}}{I} = \frac{M_{\max} \left(\frac{h}{2}\right)}{I} = \frac{6PL}{bh^2} \text{ (MPa)}$$

The first specimen was tested at high peak stress. This was a common procedure carried out at the point, where failure

was expected in a short number of cycles. The test stress was reduced for each successive specimen by the reduction of cantilever deflection as shown in (Table 3). The failure result of each specimen was also recorded and repeated three times in order to determine the effect of surface quality of specimens subjected in two different stages of surface improvement and to compare the results as showed in (Table 4).

4- Results:

Table 3: shows beam cantilever data analysis.

No,S	L(mm)	h(mm)	b(mm)	I(mm) ⁴	δ (mm)	P(N)	M max (Nm)
1	40	1.03	10.1	0.9197	9	77.599	3.10398
2	40	1.03	10.1	0.9197	8	68.978	2.75913
3	40	1.03	10.1	0.9197	7	60.356	2.41424
4	40	1.03	10.1	0.9197	6	51.733	2.06935
5	40	1.03	10.1	0.9197	5	43.111	1.72445
6	40	1.03	10.1	0.9197	4	34.489	1.37956
7	40	1.03	10.1	0.9197	3	25.866	1.03467
8	40	1.03	10.1	0.9197	2	17.244	0.68978

Table 4 :The average results of fatigue lifetime of specimens at various amplitude, subjected to varying surface finish techniques.

No of Samples	δ (m m)	σ max (MPa)	Fatigue lifetime (number of cycle)					
			As fabricated material		Re-melted material		Polished material	
			No of cycle	Error	No of cycle	Error	No of cycle	Error
1	9	1738.2	1618	110	2046	258	2272	319
2	8	1554	3302	231	4274	408	4843	556
3	7	1351.9	5476	175	7572	746	7733	781

4	6	1158.8	9623	387	11575	979	12706	877
5	5	965.6	19067	454	24913	2328	29009	3499
6	4	772.5	42028	1787	55738	4136	63601	5305
7	3	579.4	82229	3780	103503	7551	133627	10239
8	2	386.6	200000		200000		200000	

5- Discussion :

It is important to a expand the knowledge related to material properties of additive manufacture fields in order to broaden the field of component application. The dynamic mechanical be heavier (fatigue lifetime)of the SLM components have been surveyed through different three stages of surface qualities as shown in the followed (Figure 9).

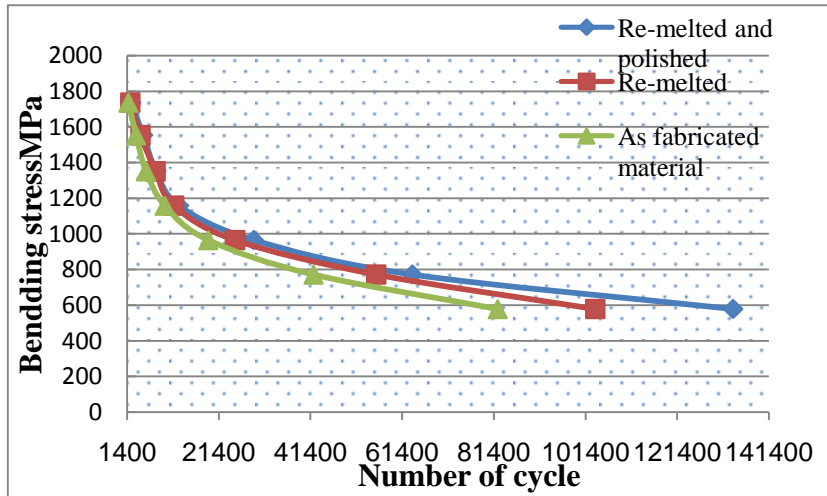


Figure 9: Stress-carve lifetime for tested material at different deflection.

The S-N relationship was obtained for various specific loading amplitudes and created for the materials tested under varying stress amplitude. The stress amplitude is denoted by

'S', while the number of cycles are denoted by 'N'. There were various drawbacks in the S-N fatigue data. Firstly, the actual service conditions of test specimens did not present the same conditions, but showed different scattering of fatigue life time. Although all the specimens have been made by the same parameters see (Table 1) and exposed to the same stages of surface finish improvement they showed different results from one sample to another. These differences led to an important change in the fatigue performance, generated as a result among the samples. The demonstrated results of fatigue test are highly sensitive to the a number of tested material. Moreover, it showed considerable amount of scatter in the fatigue lifetime data, especially at lower stress, whereas less scatter was recorded at high stress (see error in Table 4). This occurs in spite of the fact that the specimens were carefully made and treated.

From the results observed in the above plotted (S-N) curve, the increase in fatigue lifetime is associated with decrease of the loading applied on the specimens. At higher stress, the lifetime is significantly lower for these materials even under different surface conditions, and it hasn't shown significant scattering for the three tests.

The re-melted samples with surface roughness (Ra) $1.4 \mu\text{m}$ demonstrated significant fatigue lifetime particularly at lower stress and recorded about 30% improvement in comparison with those samples fabricated by SLM. In such case, it is possible to say that laser re-melting plays a significant role in improving the behavior of the fatigue lifetime of SLM components due to its ability to suppress any dendrite, pitting, porosity and residual stress could be initiated during the manufacture process. Also providing a homogenous surface with fine microstructure is important.[13].

For re-melted and polished specimens with surface roughness (Ra) $0.35 \mu\text{m} \pm 15\%$, the effect of surface quality, failed to produce significant effects in the lifetime at higher amplitudes of stress, when compared to the behavior of re-melted material. This could be due to the high stress of applied load leading to a reduced crack growth period. However, an improvement in the fatigue lifetime has been recorded at lower stress. The results showed about 19% improvement comparable to previous re-melted samples. The reason behind this is the

fatigue lifetime to failure depends on two periods, the crack initiation period and the crack growth period. In the case of polished surfaces, the crack nucleation on the metal surface is too small leading to an increase in the initiation period. Also the period of crack growth will be larger and covers the period of crack initiation.

5.1- Macroscopic characteristic:

The observations of fatigue failure of an SLM component can be initially observed by the naked eye and it is also advised to look at with small magnification. For instance, EG 2X 4X etc. This is in order to clarify details regarding to crack nucleation and surface damage during loading. The details of defects may be major in estimating the fatigue problem.

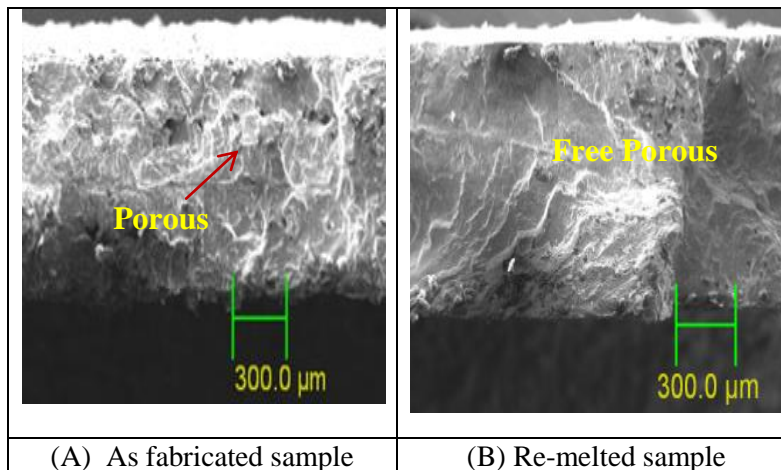


Figure 10: Micrograph of different fracture surfaces of different specimens at high stress 1350 MPa, for SLM part as fabricated (Ra= 10μm) and re-melted sample (1.5 μm)

Figure 10) shows fracture surfaces of specimens which have been obtained by SEM at low magnification. It was indicated that the fracture surface of specimens are different among the test due to the different of surfaces treatment condition. For specimens (Figure 10-A) with surface roughness (As fabricated and Ra=10μm) high number of defects on the

surface(rough and porous) leads to raising stress at the loading point, which demonstrated the reason for fast failure. In such case, cracks can initiate at any points, where high stresses increase.

On the other hand, the possibility of cracks initiation are less than for re-melted and polished samples(Figure 10-B), surface roughness ($R_a= 1.4\mu\text{m}$ & $0.35\mu\text{m}$).This due to the surfaces being more flat and having reduced porosities, leading to decrease of stress raiser and surface roughness improvement.

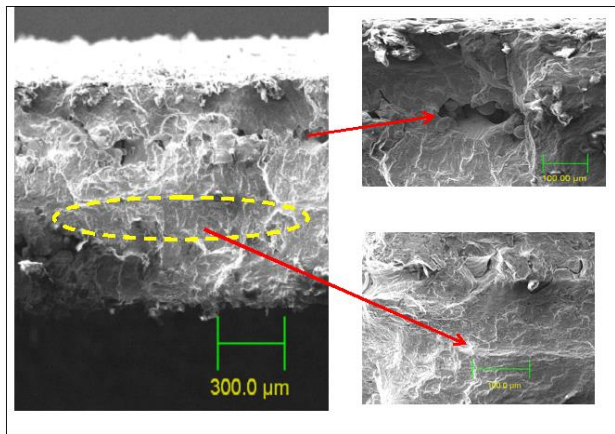


Figure 11 : Micrograph of fracture fatigue surfaces at high stress 1350 MPa for SLM part as fabricated ($R_a= 10\mu\text{m}$) to demonstrate different region of fatigue fracture surfaces.

Figure 11) shows that there are two regions in the fracture, as fabricated specimen. The first region is caused by the fatigue crack growth (out of circle in Figure 11) occurred in each cycle. As a result of the fatigue occurs by micro crack growth, a number of micro-cracks can be developed successfully on the surface and generate a large quantity of deformation. This could be enough to explain quick failure. The second region of fracture surface is that when the final cross section of specimen cannot longer carry the final applied load, leading to final fracture. In the case of SLM component, failures associated with fatigue and stress is commonly initiated by degradation on the surface, number of porosities and intensity

of externally applied load. These problems can be reduced by laser re-melting leading to extending the lifetime of the material[14].

On the other hand, many conventional surface engineering techniques are available to solve this issue, and unlike the rest, laser re-melting is regarded as the most suitable method due to its flexibility to improve surface roughness, eliminate porosity, increasing fatigue and minimizing residual stress. This is the reason why cracks have never been easily initiated in a properly re-melted surface[15],[16].

Sun and co-authors has reported that improved wear and friction resistance of a stainless steel material surface has mostly been attributed to residual compressive stress and porosities removal from a material achieved through re-melting process .Furthermore, laser re-melting has been considered more effective in improving the material surface lifetime of stainless steel as well as to enhance corrosion and oxidation resistance[17],[18].

6- Conclusion :

The potential of surface finish which affects the fatigue life time of e surveyed samples showed various response. These variations are associated with different surface roughness due to the stages of improvement(both re-melting and polishing process).

The results of the study can be sum arised in the following points:

1. The change in amplitude is an influence on the variability in the fatigue lifetime of the samples.
2. The remaining defects (high surface roughness and porosity) associated with the manufactured 316L stainless steel made by SLM specimens, are a major factor affecting the fatigue lifetime.
3. Laser re-melting improves the fatigue lifetime of SLM stainless steel 316L about 30% at lower stress. The reasons behind that are the ability to supress surface roughness, porosity issues and reduce residual stress.
4. Electro-polishing after laser re-melting results in further improvement of fatigue lifetime and resulted about 19% at lower stress.

5. In both re-melted and polished samples failed to produce significant effects in the lifetime at higher amplitudes when compared to the behavior of as-fabricated samples.
6. The improvement of fatigue lifetime by laser re-melting and later Electro-polished can be attributed to the reduction of porosity issues, surface roughness and residual stress.

References :

- [1] T. R. Thomas, Surface roughness, Imperial College Press, 2nd ed. London, 1999.
- [2] U. Khandy, "optimization of surface roughness removal, department of mechanical engineering, national institute of technology. India.," 2009.
- [3] L. Roy and V. Bhamidipati, "An Efficient Method to Estimate the S-N Curves of Engineering Materials," no. 2, pp. 2–5, 2002.
- [4] E. Yasa, J.-P. Kruth, and J. Deckers, "Manufacturing by combining Selective Laser Melting and Selective Laser Erosion/laser re-melting," CIRP Ann. - Manuf. Technol., vol. 60, no. 1, pp. 263–266, Jan. 2011.
- [5] S. M. Beden, S. Abdullah, and A. K. Ariffin, "Review of Fatigue Crack Propagation Models for Metallic Components," Eur. J. Sci. Res., vol. 28, no. 3, pp. 364–397, 2009.
- [6] P. C. Paris and F. Erdogan, "A Critical Analysis of Crack Propagation Laws," J. Basic Engng, vol. 85, pp. 528–534, 1973.
- [7] P. C. Paris, M. . Gomez, and W. . Anderson, "A Rational Analytic Theory of Fatigue," Trend Eng., 1961.
- [8] R. G. Forman, "Study of Fatigue Crack Initiation from Flaws Using Fracture Mechanics Theory," Engng Fract. Mech, vol. 4, pp. 333–345, 1972.
- [9] E. S. Gadelmawla, M. M. Koura, T. M. A. Maksoud, I. M. Elewa, and H. H. Soliman, "Roughness parameters,"

- J. Mater. Process. Technol., vol. 123, no. 1, pp. 133–145, Apr. 2002.
- [10] B. P. Novovic D, Dewes RC, Aspinwall DK, Voice W, “Effect of machined topography and integrity on fatigue lifetime,” *Int J Mach Tools Manuf*, vol. 44, pp. 125–34, 2004.
- [11] A. B. Spierings, T. L. Starr, and K. Wegener, “fatigue performance of additive manufactured metallic parts,” *Rapid Prototyp. J.*, vol. 19, no. 2, pp. 88–94, 2013.
- [12] J. M. Gere and B. J. Goodno, *Mechanics of Materials*, 8th ed. Canada: Cengage Learning, 2012.
- [13] K. Alrbaey, D. Wimpenny, R. Tosi, W. Manning, and A. Moroz, “On optimization of surface roughness of selective laser melted stainless steel parts: A statistical study,” *J. Mater. Eng. Perform.*, vol. 23, no. 6, pp. 2139–2148, 2014.
- [14] J. a. Francis, H. K. D. H. Bhadeshia, and P. J. Withers, “Welding residual stresses in ferritic power plant steels,” *Mater. Sci. Technol.*, vol. 23, no. 9, pp. 1009–1020, Sep. 2007.
- [15] D. S. Mankar and P. V Jadhav, “effect of surface roughness on fatigue lifetime of machined component of inconel 718,” *Int. J. Fatigue*, vol. 41, no. 6, pp. 141–149, 2007.
- [16] G. Haijun, R. Khalid, and S. Thomas, “Effect of Defects on Fatigue Tests of As-Built Ti-6Al-4V Parts Fabricated By Selective Laser Melting,” in *Solid Freeform Fabrication Symposium*, 2012, pp. 499–506.
- [17] Y. Sun, A. Moroz, and K. Alrbaey, “Sliding wear characteristics and corrosion behaviour of selective laser melted 316L stainless steel,” *J. Mater. Eng. Perform.*, vol. 23, no. 2, pp. 518–526, 2014.
- [18] F. Vollertsen, K. Partes, and J. Meijer, “State of the art of Laser Hardening and Cladding,” in *Proc. of the Third Int. WLT-Conf. on Lasers in Manufacturing*, Munich, AT-Verlag, Munich, AT-Verlag, 2005.